



Deliverable D4.11

Fourier-Hankel/Legendre pipeline

G. Vigeesh, H.-P. Doerr, K. Glogowski, and M. Roth

Kiepenheuer-Institut für Sonnenphysik, Schöneckstrasse 6, 79104
Freiburg, Germany

1 Introduction

The Sun oscillates as a result of ringing by trapped acoustic waves that are stochastically excited by turbulent convection. These oscillations permeate the solar envelope and can be measured on the solar surface. They provide an invaluable source of information allowing us to probe beneath the surface. Helioseismology is the field of research that uses these oscillations to determine the internal properties of the Sun. As continuous spatially resolved data became available from ground (GONG) and satellite-borne instruments (SOHO/MDI, SDO/HMI), the field of helioseismology progressed considerably over the last 50 years, developing new techniques and improving our understanding of the Sun.

Of the several techniques currently in use in local helioseismology (*Ring-diagram analysis*: Hill (1988), *Time-distance analysis*: Duvall et al. (1993) *Acoustic holography*: Lindsey & Braun (1998)), the Fourier-Hankel spectral decomposition was one of the earliest techniques used by helioseismologists to explore the subsurface regions of the Sun. It was first employed by Braun et al. (1987), and later followed up by a series of work (Braun et al., 1988; Braun & Duvall, 1990; Braun et al., 1990, 1992) to study the interaction of solar acoustic modes (p -modes) with isolated large scale magnetic structures like sunspots. Sunspots are local discontinuities in the near surface regions of the Sun. The p -modes sample these discontinuities and leave signature of their interaction on the oscillation spectra. Whereas, the spectra of the modes that have not encountered the sunspot remains unaltered. Fourier-Hankel method can be used to separate these two wave fields. This is done by decomposing the wave field into radially inward and outward propagating waves on an annular region centered in the sunspot. It was observed that the power in the outgoing wave was significantly less compared to the ingoing wave suggesting that the sunspot “absorbs” these p -modes. The absorption depended on the horizontal wave number and the outgoing wave showed significant phase-shift compared to the ingoing wave.

Although, Hankel functions are good approximations, later studies also explored this method with the help of associated Legendre functions to account for the curvature of the solar surface. The results of Bogdan et al. (1993), were consistent with the earlier studies but found discrepancies in absorption at large wave numbers, which they ascribed to the reduced lifetime and spatial range of p -modes that live near the surface. These observations motivated further research towards explaining the absorption of p -modes by sunspots and different mechanisms were proposed, including dissipation due to the intrinsic properties of the sunspot (La Bonte & Ryutova, 1993), mode-conversion (Spruit & Bogdan, 1992), mode-mixing (D’Silva, 1994), etc. It is now believed that the absorption and the scattering phase-shifts seen in sunspots are the result of the p -modes interacting with the magnetic field and undergoing mode-conversion into other magneto-acoustic modes (Cally & Bogdan, 1997; Cally et al., 2003).

The application of Fourier-Hankel/Legendre technique was later extended to other helioseismic studies. Braun & Fan (1998) carried out meridional flow measurements using this technique by decomposing the wavefield into equatorward and poleward wavefields and measuring the frequency shifts between them. However, they were unable to find evidence for a return flow

even down to a depth of 30 Mm. Since an equatorward return flow is a major ingredient in dynamo models, helioseismic measurements are needed to establish the actual profile of meridional circulation. Further work carried out by Krieger et al. (2007) and Doerr et al. (2010) in this direction have resulted in the development of a fast and efficient code for the computation of Fourier-Hankel/Legendre transform which can be easily applied to a large amount of data (Glogowski, 2011). Preliminary results for meridional flow obtained from this work are comparable to the results obtained using ring-diagram analysis.

Meanwhile, researchers shifted their focus on more general techniques like time-distance and ring-diagram analyses as more data became available. However, recent work using data from SDO/HMI and AIA instruments have revived the Fourier-Hankel method and have used them to study wave propagation in the solar atmosphere. Couvidat (2013) looked at different layers of the solar atmosphere above several sunspots and quiet Sun regions to study the absorption and scattering of surface gravity waves (f -mode) and p -mode oscillations. Couvidat (2014) find that the absorption shows a significant dependence on height, whereas the phase-shift does not, which again confirm the mode-conversion scenario explained by Cally et al. (2003). Fourier-Hankel techniques have been applied to numerical data to study the scattering of f - and p -modes by different magnetic structures in an attempt to understand the anatomy of sunspots (Felipe et al., 2012, 2014).

As the demand for Fourier-Hankel/Legendre analysis is rekindled, a fast and automated data processing tool to process the available and future data is vital. While there are fully developed pipeline modules for other helioseismic techniques, a module for the Fourier-Hankel/Legendre spectral decomposition and analysis is not available. In this work, we have implemented a Fourier-Hankel/Legendre module on the SDO/HMI JSOC data-analysis pipeline for processing large sets of HMI data, based on an existing code developed by Doerr et al. (2010). We present here the details of the pipeline module.

2 Fourier-Hankel/Legendre spectral decomposition

Given a cylindrically symmetric velocity field (δV) on a surface, the underlying wave field can be described as a superposition of waves propagating radially inward and outward. These two components can be expressed in

terms of Hankel functions of the first and the second kind. The two Hankel functions are linear combination of Bessel functions of the first and second kind that lie on a (r, ϕ) grid, where r is the arc-length and ϕ is the azimuthal angle, with the corresponding wavenumbers represented by k and m , respectively. Considering a spherical symmetric case like the Sun, these functions can be easily mapped onto the surface of a sphere (θ, ϕ) by identifying the center of the cylindrical coordinate with one of the poles of the local spherical coordinate system, thus, $r = R_{\odot}\theta$ and $\phi = \phi$, where θ and ϕ are the polar and the azimuthal angle. The horizontal wavenumber corresponding to the latitudinal component is now described by the spherical harmonic degree l , such that, $k = \sqrt{l(l+1)}/R_{\odot}$. Hence, the velocity field on a local spherical surface can be described as,

$$\delta V_z(\theta, \phi, t) = \sum_n \sum_{l \geq 0} \sum_{|m| \leq l} \left[A_{lm}(t) H_m^{(1)}(\sqrt{l(l+1)}\theta) + B_{lm}(t) H_m^{(2)}(\sqrt{l(l+1)}\theta) \right] e^{i(m\phi + \omega_n t)}, \quad (1)$$

with the phase factor $e^{im\phi}$ modifying the Hankel functions along the ϕ direction. The two Hankel functions are defined as,

$$H_m^{(1)}(kr) = \left[J_m(kr) + iY_m(kr) \right], \quad (2)$$

$$H_m^{(2)}(kr) = \left[J_m(kr) - iY_m(kr) \right], \quad (3)$$

where J_m and Y_m are the Bessel functions of the first and second kind, respectively.

The complex coefficients, A_{lm} and B_{lm} , describe the amplitude of the oppositely directed wave modes of degree l and azimuthal order m . Hankel functions are particularly suited for sunspot seismology and local analysis that take into account only the cylindrical symmetry of the problem (see Fig. 1). In order to study large scale flows, like the meridional circulation, a more judicious choice is to rotate the local spherical coordinate to match with the solar poles. This allows us to exploit the effect of the meridional flow on the wave field by decomposing it in terms of poleward and equatorward wave modes. For such cases, Hankel functions are not a good approximation, as the function falls off with large kr , or towards low heliographic latitudes, rendering them less suitable for analysis of larger areas, far away from the poles.

Associated Legendre functions are the natural extension to Bessel functions to describe the wave field on the surface of a sphere. This makes them

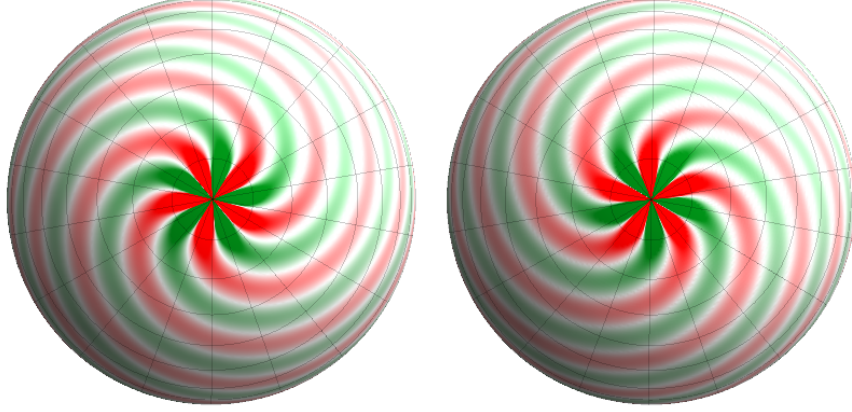


Figure 1: Hankel functions modified by a phase factor are used to describe the inward and outward propagating wave field. The figure shows the real part of the functions mapped on a sphere, $H_m^1(\sqrt{l(l+1)}\theta)e^{im\phi}$ (left) and $H_m^2(\sqrt{l(l+1)}\theta)e^{im\phi}$ (right) for $l = 20$ and $m = +5$, with the coordinate system centered at the center of the region of interest, for e.g. the center of a Sunspot.

more useful for the study of meridional flow, by allowing one to study areas even in lower heliographic latitudes. Constructing a function, Θ_l^m , using the associated Legendre functions of the first and second kind (P_l^m and Q_l^m) as,

$$\Theta_l^m(\theta, \phi) = \sqrt{\frac{2l+1}{4\pi} \frac{(l-m)!}{(l+m)!}} \left[P_l^m(\cos\theta) - \frac{2i}{\pi} Q_l^m(\cos\theta) \right], \quad (4)$$

the velocity field can be described in the following way,

$$\delta V_z(\theta, \phi, t) = \sum_n \sum_{l \geq 0} \sum_{|m| \leq l} \left[A_{lm}(t) \Theta_l^m(\theta, \phi) + B_{lm}(t) \overline{\Theta_l^m}(\theta, \phi) \right] e^{i(m\phi + \omega_n t)}, \quad (5)$$

where, $\overline{\Theta_l^m}$ is the complex conjugate of Θ_l^m . The coefficients, A_{lm} and B_{lm} , describe the amplitude of the poleward and equatorward wave modes of degree l and azimuthal order m , when the coordinate systems is centered at the solar poles (see Fig. 2).

Thus, depending on what one intends to study, the Dopplergrams are mapped onto the appropriate grid and decomposed to obtain the amplitudes

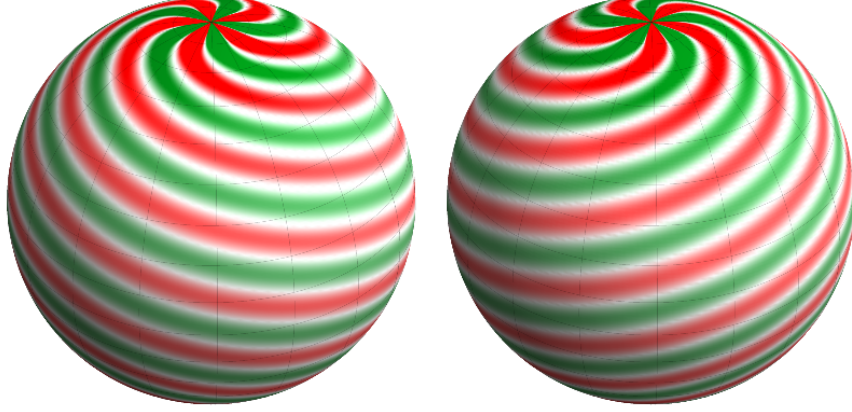


Figure 2: Combinations of associated Legendre functions of the first and second kinds are used to describe the poleward and equatorward propagating wave field. The figure shows the real part of the function $\Theta_l^m e^{im\phi}$ (left) and $\overline{\Theta}_l^m e^{im\phi}$ (right) for $l = 20$ and $m = +5$, with the coordinate system centered at the solar poles. Unlike the Hankel functions, the Θ_l^m does not drop as one gets to lower heliographic latitudes.

of the inward and outward propagating wave modes as,

$$A(l, m, t) = \frac{\sqrt{l(l+1)}\pi}{2\Theta} \int_{\Phi_{\min}}^{\Phi_{\max}} \int_{\Theta_{\min}}^{\Theta_{\max}} v(\theta, \phi, t) \overline{F}_l^m(\theta) e^{-i(m\phi + \omega_{nl}t)} d\Theta d\Phi, \quad (6)$$

$$B(l, m, t) = \frac{\sqrt{l(l+1)}\pi}{2\Theta} \int_{\Phi_{\min}}^{\Phi_{\max}} \int_{\Theta_{\min}}^{\Theta_{\max}} v(\theta, \phi, t) F_l^m(\theta) e^{-i(m\phi + \omega_{nl}t)} d\Theta d\Phi, \quad (7)$$

where F_l^m is either the Hankel function $H_m^{(1)}(\sqrt{l(l+1)}\theta)$ or the Θ_l^m . The module described here, carries out the above decomposition. Description of how these decomposition is carried out in the module is described in the later section.

3 The pipeline

The large amount of data delivered by the different instruments onboard the Solar Dynamics Observatory (SDO) are managed by a data management system developed by the Joint Science Operations Center (JSOC).

The main component of this system is the Data Record Management System (DRMS), which is used to process, archive, and distribute data (Bogart, 2007). The data, available at different stages of processing, are all handled by the DRMS which groups them into different *data series* based on the common properties of the data (like the instrument, the physical quantity e.g. Dopplergrams, Tracked cubes, SHT coefficients, etc.). Within each *data series*, the individual datasets are identified as *data records*. A set of primary keywords are used to describe these common properties which can then be used to access/query the data. The actual data is stored separately in the Storage Unit Management System (SUMS). In order to communicate with the database, there is an Applications Programming Interface (API). Within this architecture, a pipeline module interacts with the DRMS and SUMS to retrieve data from the database and processes it and stores back the processed data into the database for further analysis. The interaction with the database is facilitated by the API available to the pipeline module writer. There are several pipeline modules available for different standard products, such as a set of modules that work in succession to finally give out the subsurface velocity maps using the Ring-diagram analysis technique. Most of these modules are meant for their specific flow and are hardly ever used by other techniques. In this work, we have used one of the modules, `mtrack`, adapting it to suit our purposes and we also have extensively utilised the API provided by JSOC and in some case modified them to suit our purpose. The current version of the module can be used for meridional flow measurements and also for sunspot seismology.

3.1 Installation

Unzip the archive to the local directory and edit the Makefile with the appropriate paths to CFITSIO and HDF5.

```
make
```

Make produces three executables: `postel_remap`, `tld`, `fld`.

In the following, we describe the working of the pipeline and how to use the module along with other standard modules.

3.2 The pipeline workflow

The Fourier-Legendre analysis are usually performed on small areas of the solar surface to infer the average properties beneath the selected region. For instance, to estimate the meridional flow as a function of latitude, rectangular patches are extracted from the Dopplergram images in the North-South direction along a specific longitude (usually the Stonyhurst $\phi = 0^\circ$), centered at different latitudes. The Fourier-Hankel/Legendre decomposition gives the amplitude of the poleward and equatorward directed flow field. The difference in frequency between these two oppositely directed components can be attributed to a Doppler shift as a result of a flow in a particular direction. Assuming that the origin of this flow is due to the meridional circulation, the frequency shifts can be inverted to get the magnitude of the meridional flow at different depths as a function of latitudes. For sunspot seismology, annular regions are selected centered in the spot and the decomposition gives the amplitude of the ingoing and outgoing waves within this annulus. The absorption coefficients and scattering phase-shifts can then be estimated from the amplitude of the two components. It should be noted that, for the meridional flow measurements the center is fixed on one of the poles, while in the case of sunspot it is the spot center. In both cases, the decomposition is carried out on an equi-angular grid and therefore the first step is to select the region of interest and map it onto an appropriate grid.

Mapping and Tracking

The mapping and tracking of the desired region can be performed by the module `mtrack`, which is a standard module used by other helioseismology pipeline modules. In order to use `mtrack` and store the tracked data cubes of velocity as a function of Carrington Latitude (Θ), Longitude (Φ), and time (t): $V_z(\Theta, \Phi, t)$, a new data series needs to be created in the DRMS. This data series can be created using a JSOC series definition (JSD) file. A template for creating a data series for storing `mtrack` dataset that can be used by the following modules in the Fourier-Hankel/Legendre analysis pipeline is available under `kis_vigeesh.hmi_fldvtrack.jsd`. The series definition file contains the general series information where the primary keys are specified. The `Keywords` section contains the secondary keys and the `Segment` section contains the details of the data segment that the data series actually stores in the SUMS. For our purposes, the series definition file slightly differs from one than that is normally used by other techniques which are mainly intended for standard data products. In the case of a standard data

series, one usually specifies the final pixel size and the total duration of the mapped and tracked cube. This module is intended to be used for specific analyses and hence there is no need to specify the final pixel size and the time-length of the tracked data and therefore one can set these keywords to a **variable**. This allows us the freedom to choose the size of each data cube at runtime, rather than constraining it to a specific size.

The module `mtrack` is used to map the data from heliocentric-cartesian projection to a Carrington heliographic or a Postel projection. An explanation on the different projections and transformation used in processing images are described in Thompson (2006). The primary input to the module `mtrack` are the full-disk Dopplergrams available as the data series `hmi.v_45s`. The region to be mapped and tracked is described by the Heliographic Latitude (Θ) and Longitude (Φ) of the central pixel and the width and height of the whole region in pixels. This is passed to the module using the `lat` and `lon` arguments. It should be noted that the `lon` is specified in Carrington coordinates and not Stonyhurst. The total number of pixel-rows and columns of the mapped region are passed using the `rows` and `cols` argument. The final resolution of the image is specified using the `scale` argument, which sets the desired `Mapscale` in degrees/pixel. The decomposition module can process Plate Carrée or Postel map projection, and hence the `map` argument can be set to either `'carree'` or `'Postel'` depending on whether one intends to use it for meridional flow measurements or sunspot seismology. The tracked output will be stored in the data series that we just defined using the JSD file. A new series is created using the `create_series` command as follows,

```
create_series kis_vigeesh.hmi_fldvtrack.jsd
```

Once the series is created in the DRMS, we can use the pipeline modules to populate the series with data records. Here we show an example usage to generate an untracked region centered at $(\Theta, \Phi) = (0, 200)$ spanning 8 hours, with the line-of-sight component of observer velocity and the solar rotation removed,

```
mtrack in='hmi.v_45s[2010.06.01_00:00:00_TAI/8h]' \
      out='kis_vigeesh.hmi_fldvtrack' \
      scale=0.125 lat="{0.}" lon="{200.}" \
      map="carree" rows=400 cols=400 -n -v -o -r
```

In the above example, regions are mapped onto plate carrée projection, in which the heliographic longitude and the latitude are equally spaced in degrees. The solar rotation is tracked at the Snodgrass rate with only the \sin^2 term. The flag `n` turns off tracking, only correcting for the anomalous observer motion ($a_0 = -2.8653291$, $a_2 = a_4 = \text{merid_v} = 0$). The flag `o` removes the line-of-sight component of observer velocity and `r` removes the line-of-sight component of solar rotation. To generate multiple sets of tracked regions the `lat` and `lon` keywords can be given as lists. For instance, `lat="{0.,10.,20.,30.,40.}" lon="{200.,190.}"` creates data records containing maps centered at $(\Theta, \Phi) = (0., 200.)$, $(10., 210.)$, $(20., 190.)$, $(30., 190.)$, $(40., 190.)$, within the same output data series.

In order to study active-region patches, the Dopplergrams are usually tracked and projected onto a Postel grid. In order to process these maps, the Fourier-H/L module first remaps the Dopplergrams onto a rectangular grid. Further details of how the Postel maps are handled by the decomposition module is explained in the next section. An example below shows how a Sunspot (AR 11084) is tracked and mapped on to a Postel projected map and stored in the DRMS.

```
mtrack in='hmi.v_45s[2010.07.02_12:00:00_TAI/8h]' \
      out='kis_vigeesh.hmi_fldvtrack' \
      scale=0.125 lat="{0.}" lon="{200.}" \
      map="Postel" rows=400 cols=400 -v -o -r \
      a0=-0.02893 a2=-0.3441 a4=-0.5037
```

In both the above examples, the data cubes are stored as fits files inside the SUMS that can be viewed using the `show_info` command.

```
show_info \
  kis_vigeesh.hmi_fldvtrack[2010.06.01_00:00:00_TAI/5m] \
  -P key=MidTime,LonHG,LatHG,Duration
```

In order to use the data series with the rest of modules in the pipeline, certain essential keywords are needed. These are the: `MidTime`, `LonHG`, `LatHG`, `Duration`, `Cadence`, `MapScale`, `MapProj`, `Width`, `Height`, and therefore these keywords needs to be specified in the series definition file. The keyword `MidTime` gives the mid time of the tracked data cube. A 16 day long data cube starting on 2010.06.01 created using `mtrack` using the argument `in='hmi.v_45s[2010.06.01_00:00:00_TAI/16d]'` will acquire a

value 2010.06.08_00:00:00_TAI for `MidTime`. Unlike all the other data series where the `T_START` is the primary keyword, all the follow-up modules use the new `MidTime` as a primary keyword in order to retrieve/query the data from the database.

Fourier-Hankel/Legendre time series

The next module in the Fourier-Hankel/Legendre pipeline is the `tld` module that reads in the Dopplergrams and performs a spatial decomposition and gives out the Fourier-Hankel/Legendre time series. The `tld` module queries the input series, which are the mapped and tracked data cube created using the `mtrack`. The relevant keywords that describe the data, as explained in the previous section, are passed on from the input series. The user is required to supply the maximum l and the absolute maximum m that is desired. The final time series will then contain the Fourier-Hankel/Legendre coefficients from $l = 0$ to l_{\max} and $m = -m_{\text{abs}}$ to m_{abs} for a given map centered at (θ, ϕ) . Presently, the code can only process individual sets of (θ, ϕ) maps. The main decomposition is carried out on an regular equi-angular grid, without including the poles, and therefore the Dopplergrams are required to be mapped onto this grid. If the mapped data is on “PlateCarre” projection, the decomposition is directly carried out, but if the data is “Postel” projected then a remapping has to be performed on the data. The accompanying module `postel_remap` can be used to stretch the map along the azimuthal and radial direction (as shown in Fig. 3) before carrying out the decomposition.

In order to run the decomposition module in the pipeline form, a new data series has to be created that can store the Hankel/Legendre coefficients. The output of the module are 3 dimensional complex arrays of the two coefficients corresponding to the inward and outward propagating wave, *viz.* $A(l, m, t), B(l, m, t)$. In the case of other pipeline modules, like the global SHT, the transformed coefficients are stored by chunking in l . While this is possible in our case, this would restrict the user by allowing only up to a certain predefined l to be stored in the database. In order to store the whole array up to the desired l arrays into the DRMS, the output data format is set to ‘`generic`’, since the output file format is now ‘`hdf5`’ instead of ‘`fits`’, although there is an option to output the data into FITS files. The reasons for using the Hierarchical Data Format version 5 (HDF5) file format is for generality and the ease of parallel-processing. Since the number of l, m are not predefined in the series definition, and since we need to

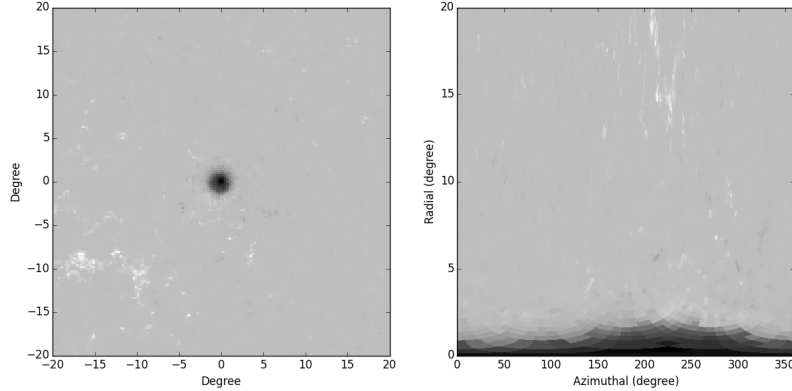


Figure 3: A representative image showing how the remapping to a equiangular grid is performed prior to decomposition of a Postel projected map. Left: The Postel projected magnetogram map centered at active region, AR 11084. Right: The map on the left side is stretched and remapped on a equiangular grid, along arc-length and azimuthal angle, before decomposition.

have the flexibility in choosing these values at runtime, we thought it would be appropriate to use a file format like HDF5. This also allows us to avoid storing multiple files (A, B) under the same data record and consolidating them into a single file. Yet another reason why we chose to go with the new file format is parallel I/O is not yet supported for FITS file, which would generate again multiple files for each coefficients depending on the number of processors used under the same data record. And finally, having a single file allows us to access the time series for l, m , as we now have access to hyperslabs of data within the HDF5 container, making it less memory and I/O intensive. A template for creating the data series to store the transformed coefficients is available under `kis_vigeesh.hmi_tldcoeff.jsd`.

Once the new series is created, and the tracked data record is available in the appropriate series, the decomposition can be performed as follows,

```
mpirun -np 12 tld \
  in=kis_vigeesh.hmi_fldvtrack[2010.06.01_00:00_TAI][+200][0] \
  out=kis_vigeesh.hmi_tldcoeff m_abs=25 l_max=1000 \
  decomp='FLD' apdof='Tukey' apodw=8
```

The module is parallelised using Message Passing Interface (MPI) in order to process the data cube by splitting them into smaller chunks along the time axis. The master reads in the input record and checks for a data set with a rank 3. The master also reads in the necessary keywords and most importantly checks for the map projection. The velocity data available in the input record is then read in. If the map projection is Postel, a remapping is performed before dividing the whole data into chunks along the time axis, the number of chunks depend upon the number of processors assigned. The master processor creates the output record and opens a HDF5 container file in the local directory and adds in the `Alm` and `B1m` data spaces to the `/lmg` group. The master then assigns the divided chunks to the respective slaves. Each slave processor gets a small part of the whole data cube and the decomposition is performed. For each map in the chunked time series, a low pass filter is applied with an FWHM given by `lowpass_fwhm`. The maps are then apodized using the different window functions available: `Tukey`, `Hann`, `Hamming`, `Cosine` with the width of the apodization window passed on by the `apodw` argument. The maps are now ready for the Hankel/Legendre transformation. The transformation to be performed is provided by the `decomp` argument. Depending upon Hankel or Legendre, the basis functions are generated on the equi-angular grid and stored.

The Hankel basis functions are calculated in their asymptotic limit ($\theta \gg 1/L$) as,

$$H_m^{(1)}(kr) = \sqrt{\frac{2}{\pi kr}} e^{i(kr - \pi/4 - m\pi/2)}, \quad (8)$$

$$H_m^{(2)}(kr) = \sqrt{\frac{2}{\pi kr}} e^{-i(kr - \pi/4 - m\pi/2)}, \quad (9)$$

where, $kr = \sqrt{l(l+1)}\theta$, when projected on the surface of a sphere. The module uses Eq. 8-9 to calculate the basis functions when the decomposition is set to `FHD`.

The associated Legendre polynomials are calculated using their recurrence relations. The recurrence relations provide a reliable method for computing the basis function, although not every recurrence relation is numerically stable. In the following, we provide a summary of the method that is used to calculate the associated Legendre polynomials. The method and the C function that implements this is borrowed from Zhang & Jin (1996), where

it is described in more details.

The main recurrence relations used in the computation of associated Legendre polynomials are,

$$P_l^m(x) = xP_{l-1}^m(x) - (l+m-1)\sqrt{1-x^2} P_{l-1}^{m-1}(x), \quad (10)$$

$$P_l^m(x) = \frac{1}{l-m} [(2l-1)xP_{l-1}^m(x) - (l+m-1)P_{l-2}^m(x)]. \quad (11)$$

$$P_l^m(x) = -\frac{2(m-1)}{\sqrt{1-x^2}} xP_l^{m-1}(x) - (l+m-1)(l-m+2)P_l^{m-2}(x). \quad (12)$$

By taking $m = l$, a relation for $P_{l+1}^l(x)$ can be obtained from Eqs. 10 & 11,

$$P_l^l(x) = -(2l-1)\sqrt{1-x^2} P_{l-1}^{l-1}(x) \quad (13)$$

$$P_{l+1}^l(x) = (2l+1)xP_l^l(x) \quad (14)$$

since $P_{l-1}^l(x) = 0$.

Starting with $P_0^0(x) = 0$, we can compute $P_l^l(x)$ and $P_{l+1}^l(x)$ for all $l = 0, \dots, l_{\max}$ using Eqs. 13 & 14. The remaining functions, $P_{m+2}^m(x), \dots, P_l^m(x)$ can be computed from $P_m^m(x)$ and $P_{m+1}^m(x)$, using Eq. 10. Once the $P_l^m(x)$'s, for all positive m are computed, the negative m can be calculated using the relation,

$$P_l^{-m}(x) = (-1)^m \frac{(l-m)!}{(l+m)!} P_l^m(x). \quad (15)$$

Although the associated Legendre functions of the second kind, $Q_l^m(x)$, satisfy the same recurrence relations as the associated Legendre functions of the first kind, calculating them using the forward recurrence is unstable. Therefore, the computation of $Q_l^m(x)$ is carried out in a slightly different manner with the help of a backward recurrence relation.

Given, $\lim_{l \rightarrow \infty} Q_l^0(x) = 0$, we can define a function, $F_l^0(x)$, related to $Q_l^0(x)$ by a proportionality factor s_0 ,

$$Q_l^0(x) = s_0 F_l^0(x), \quad (16)$$

such that, $F_{l+2}^0(x) = 0$ & $F_{l+1}^0(x) = 1$, for some arbitrarily large value of $l = l'$. The function, $F_l^0(x)$, satisfies the same recurrence relation as $Q_l^0(x)$.

Thus, starting with $l = l'$, all the $F_l^0(x)$ till $F_0^0(x)$ can be computed using the backward recurrence relation,

$$F_l^0(x) = \frac{1}{l+1} [(2l+3)x F_{l+1}^0(x) - (l+2)F_{l+2}^0(x)] \quad (17)$$

Using $F_0^0(x)$, and the relation for $Q_0^0(x)$,

$$Q_0^0(x) = \frac{1}{2} \ln \frac{1+x}{1-x}, \quad (18)$$

we can compute s_0 , and consequently all the $Q_l^0(x)$ for $l = 1, \dots, l_{\max}$. In a similar way, all $Q_l^1(x)$ is computed. Given $Q_l^0(x)$ and $Q_l^1(x)$, the remaining polynomials up to the prescribed maximum m , $Q_l^m(x)$ can be computed using the recurrence relation given in Eq. 12. The $Q_l^m(x)$ for negative m is computed using the same way as given in Eq. 15.

The basis functions, Θ_l^m , required for the Fourier-Legendre transformation is constructed from the above P_l^m and Q_l^m using,

$$\Theta_l^m = N_l^m [P_l^m - \frac{2i}{\pi} Q_l^m] \quad (19)$$

where, N_l^m is a normalisation factor and is defined as,

$$N_l^m = \sqrt{\frac{2l+1}{4\pi} \frac{(l-m)!}{(l+m)!}}. \quad (20)$$

But the choice of N_l^m is not trivial and depends on transformation that is desired. In order to approximate the Θ_l^m to Hankel functions, one uses,

$$N_l^m = (-l)^m \frac{(l-m)!}{(l+m)!}. \quad (21)$$

Using this normalisation factor results in Θ_l^m to behave like Hankel functions for smaller values of θ , but deviate significantly for large θ and small l . The module uses Eq. 21 when the decomposition is set to FLD.

The basis functions are computed and stored in memory and the spatial decomposition is carried out according to Eqs. 6-7. As the computation is carried out on a discretely sampled equiangular grid, the integral can be written as a quadrature,

$$A(l, m) = \sum_{\theta} \sum_{\phi} q_{\theta} v(\theta, \phi) F_{lm}^*(\theta) e^{-im\phi} \quad (22)$$

$$B(l, m) = \sum_{\theta} \sum_{\phi} q_{\theta} v(\theta, \phi) F_{lm}(\theta) e^{-im\phi} \quad (23)$$

where, q_{θ} are the spherical quadrature weights. An efficient computation of Eqs. 22-23, uses the method by Driscoll & Healy (1994), which utilizes the FFT algorithm to speed up the computation. First, the azimuthal or longitudinal decomposition is performed using FFT,

$$q_m(\theta) = \sum_{\phi=\phi_{\min}}^{\phi_{\max}} v(\theta, \phi) e^{-im\phi} \quad (24)$$

for all the m 's. Then, the final Fourier-Hankel/Legendre coefficients are calculated as,

$$A(l, m) = C_l \sum_{\theta=\theta_{\min}}^{\theta_{\max}} q_m(\theta) \overline{F_l^m(\theta)} \quad (25)$$

$$B(l, m) = C_l \sum_{\theta=\theta_{\min}}^{\theta_{\max}} q_m(\theta) F_l^m(\theta) \quad (26)$$

where, F_l^m is the appropriate basis function, and,

$$C_l = \frac{\sqrt{l(l+1)}\pi}{(\theta_{\max} - \theta_{\min})}, \quad (27)$$

is the normalization constant as described in Gizon & Birch (2005).

Each processor performs the above computation on the respective chunk and then fills in the 'hdf5' container at the specific location with transformed complex values of $A(l, m, t)$ and $B(l, m, t)$. Finally, the HDF specific attributes are added and the file is assigned to the data series where it gets its own SUMS location. The master also adds in the appropriate keywords to the DRMS. The data series acquires some new keywords apart from the other keywords that are propagated from the `mtrack` module. The two new keywords are `lMax` and `mAbs`, which gives the maximum l and the absolute of the maximum m , respectively, available in the series. These keywords are then used by the next module without the need for specifying it at runtime. The data records in the new series can be queried as follows:

```
show_info kis_vigeesh.hmi_tldcoeff[2010.06.01_00:00_TAI] \
-P key=MidTime,LonHG,LatHG,Duration,lMax,mAbs
```

The Fourier-Hankel/Legendre coefficients are available in the 'hdf5' file and can be viewed using hdfview command-line tool. A simple read routine in IDL and Python is provided with this. An experimental module (`f1d`) that computes the power spectra is also provided. Like with the other modules, a template for creating the series for storing the power spectra is available under `kis_vigeesh.hmi_f1dcoeff.jsd`.

References

- Bogart, R. S. 2007, *Astronomische Nachrichten*, 328, 352
- Bogdan, T. J., Brown, T. M., Lites, B. W., & Thomas, J. H. 1993, *ApJ*, 406, 723
- Braun, D. C. & Duvall, Jr., T. L. 1990, *Sol. Phys.*, 129, 83
- Braun, D. C., Duvall, Jr., T. L., & Labonte, B. J. 1987, *ApJ*, 319, L27
- . 1988, *ApJ*, 335, 1015
- Braun, D. C., Duvall, Jr., T. L., Labonte, B. J., Jefferies, S. M., Harvey, J. W., & Pomerantz, M. A. 1992, *ApJ*, 391, L113
- Braun, D. C. & Fan, Y. 1998, *ApJ*, 508, L105
- Braun, D. C., Labonte, B. J., & Duvall, Jr., T. L. 1990, *ApJ*, 354, 372
- Cally, P. S. & Bogdan, T. J. 1997, *ApJ*, 486, L67
- Cally, P. S., Crouch, A. D., & Braun, D. C. 2003, *MNRAS*, 346, 381
- Couvidat, S. 2013, *Sol. Phys.*, 282, 15
- . 2014, *Sol. Phys.*, 289, 721
- Doerr, H.-P., Roth, M., Zaatari, A., Krieger, L., & Thompson, M. J. 2010, *Astronomische Nachrichten*, 331, 911
- Driscoll, J. R. & Healy, D. M. 1994, *Advances in Applied Mathematics*, 15, 202
- D’Silva, S. 1994, *ApJ*, 435, 881
- Duvall, Jr., T. L., Jefferies, S. M., Harvey, J. W., & Pomerantz, M. A. 1993, *Nature*, 362, 430
- Felipe, T., Braun, D., Crouch, A., & Birch, A. 2012, *ApJ*, 757, 148
- Felipe, T., Crouch, A. D., & Birch, A. C. 2014, *ApJ*, 788, 136
- Gizon, L. & Birch, A. C. 2005, *Living Reviews in Solar Physics*, 2, 6
- Glogowski, K. 2011, Diploma Thesis.

Hill, F. 1988, ApJ, 333, 996

Krieger, L., Roth, M., & von der Lühe, O. 2007, Astronomische Nachrichten, 328, 252

Lindsey, C. & Braun, D. C. 1998, ApJ, 499, L99

Thompson, W. T. 2006, A&A, 449, 791

Zhang, S. & Jin, J. 1996, Computation of Special Functions.